PHYSICAL REVIEW B **80**, 241406(R) (2009)

Electrical properties of the graphene/4*H*-SiC (0001) interface probed by scanning current spectroscopy

S. Sonde,[1,2] F. Giannazzo,[1,*] V. Raineri,[1] R. Yakimova,[3] J.-R. Huntzinger,[4] A. Tiberj,[4] and J. Camassel[4]
[1]*CNR-IMM, Strada VIII, 5 Zona Industriale, 95121 Catania, Italy*
[2]*Scuola Superiore di Catania, Via San Nullo 5/I, 95123 Catania, Italy*
[3]*IFM, Linkoping University, Linkoping, Sweden*
[4]*GES, CNRS and Université Montpellier 2, 34095 Montpellier Cedex 5, France*
(Received 12 October 2009; published 8 December 2009)

The current transport across the graphene/4*H*-SiC interface has been investigated with nanometric lateral resolution by scanning current spectroscopy on both epitaxial graphene (EG) grown on (0001) 4*H*-SiC and graphene exfoliated from highly oriented pyrolytic graphite deposited on the same substrate [deposited graphene (DG)]. This study reveals that the Schottky barrier height (SBH) of EG/4*H*-SiC (0.36 ± 0.1 eV) is ~0.49 eV lower than the SBH of DG/4*H*-SiC (0.85 ± 0.06 eV). This result is discussed in terms of the Fermi-level pinning ~0.49 eV above the Dirac point in EG due to the presence of positively charged states at the interface between the Si face of 4*H*-SiC and the carbon-rich buffer layer, which is the precursor for EG formation.

DOI: 10.1103/PhysRevB.80.241406 PACS number(s): 81.05.Uw, 68.37.Ps, 73.30.+y, 73.63.−b

The prospect of ballistic nanometer-scale electronic devices in graphene has stimulated many experimental and theoretical studies.[1,2] They have long been supported by mechanical exfoliation of highly oriented pyrolytic graphite, which is the easiest and quickest method to obtain graphene for such a scientific purpose.[3] It produces free-standing graphene sheets of very high crystalline quality, which can be deposited on several materials. The obtained flakes are typically small (from 1×1 to 100×100 μm^2) and the yield of production is extremely low. This makes the method not suitable for applications. Another recently demonstrated method is the solid-state graphitization of SiC.[4–6] It allows the production of epitaxial graphene (EG) at the wafer scale and shows better prospects for long-term industrial applications. For instance, using this technique, top gated field effect devices have already been demonstrated.[7–9] EG is obtained from high-temperature thermal treatments performed either in ultrahigh vacuum or in standard secondary vacuum or even at atmospheric pressure in an inert gas atmosphere. Both the (0001) Si and $(000\bar{1})C$ faces of hexagonal SiC polytypes (4*H* and 6*H*) have been used but large differences have been found in the structural and electronic properties of EG grown on the two faces. In particular, on the (0001) face of SiC, both experimental and theoretical studies[10–12] have shown that EG synthesis occurs through a series of complex surface reconstructions. This starts from an initial (Si-rich) $(\sqrt{3} \times \sqrt{3})R30°$ phase which rapidly converts into a second (C-rich) $(6\sqrt{3} \times 6\sqrt{3})R30°$ reconstruction when the temperature increases. This is not yet a real graphene layer but, simply, an intermediate (buried) buffer layer (C rich) with a large percentage of sp^2 hybridization.[13] This buffer layer, which may be more or less defective with more or less Si dangling bonds at the interface, has a strong influence on the electronic properties of EG on (0001) SiC. In particular, since it strongly affects the mobility of carriers, the properties of the interface between EG and this buffer layer should be experimentally investigated and compared with the properties of mechanically exfoliated and deposited graphene (DG), where—in principle—it does not play any role. This is done in this work. We present local investigations of the interface properties by measuring with a nanoscale lateral resolution the current flowing across the interface using scanning probe microscopy.[14,15] The Schottky barrier height (SBH), defined as the energy separation between the Fermi level of graphene and the edge of the majority-carrier band of SiC, is locally determined and the SBH values measured on EG/4*H*-SiC are compared with those measured on DG on 4*H*-SiC (0001) in which *no* buffer layer is present.

The starting material was an n^+-doped (0001) 4*H*-SiC substrate, 8° off axis, with a 2-μm-thick weakly doped (n^-) epitaxial layer on top. EG growth was carried out in an inductively heated reactor, operating at a minimal pressure of 5×10^{-6} mbar. The growth temperature was 2000 °C and, to lower the Si outdiffusion process, a confining Ar pressure of 1 atm was used.[5] A piece of the same 4*H*-SiC wafer (not subjected to annealing) was used as the substrate for exfoliated graphene.[16] DG on SiC was first identified by optical microscopy. Then, torsion resonance conductive atomic force microscopy (TR-CAFM) was used to measure, simultaneously, topographic and current maps on the sample surface. TR-CAFM is a dynamic scanning probe method which allows nondestructive electrical measurements from a conductive tip oscillating in a torsional or twisting mode in close proximity to the sample surface (0.3–3 nm). When a bias is applied between the tip and the sample backside, a map of the current flowing from the tip to sample surface is acquired. This noncontact method has a distinct advantage over the conventional conductive atomic force microscopy performed in contact mode because of the absence of shear forces that can be damaging for the graphene sheets. All measurements were carried out using a Veeco DI3100 AFM with Nanoscope V controller and TUNA application module. Commercially available Si n^+-doped probes with platinum (Pt) coating were used, with a typical radius of the apex of 10–20 nm.

Figure 1(a) shows a TR-CAFM current map taken on DG.

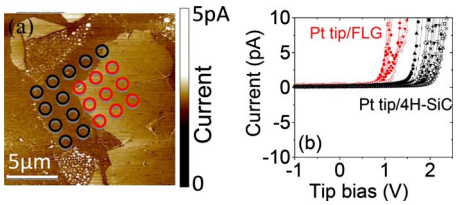

FIG. 1. (Color online) (a) Current map of DG on 4*H*-SiC (0001) at tip voltage of 1 V. The tip positions on graphene and on 4*H*-SiC are shown. (b) Typical set of SCS *I*-*V* characteristics. Two distinct families of curves are associated with the tip positions on graphene and on 4*H*-SiC.

The tip bias was 1 V. A very good correlation with the morphological map (not reported) was found, with the brighter portions in the current map (region carrying a higher current) corresponding to graphene in the morphological map. After identifying the SiC regions coated with DG, local *I*-*V* measurements were carried out by scanning current spectroscopy (SCS). In SCS the conductive tip is placed on a discrete array of positions on the sample surface noninvasively, lifting the tip by 20 nm at every interval. Thus, a continuous scan of the surface by direct contact is avoided while, at every tip position, a current-voltage (*I*-*V*) characteristic is recorded. A swift transition between TR-CAFM and SCS is possible without altering the sample position. The representative positions of the tip during the SCS scan are depicted in Fig. 1(a) and the recorded *I*-*V* curves are shown in Fig. 1(b). All *I*-*V* curves exhibit a rectifying behavior, with a low leakage current under reverse bias and a sudden increase in the current for positive bias higher than a threshold voltage. It is worth noting that the acquired curves can be divided in two groups, which correspond to the tip positions on DG and bare SiC substrate. It is clear that DG forms a Schottky contact on top of the 4*H*-SiC layer. Before examining EG for vertical current transport, Raman measurements were done to estimate the number of graphene monolayers (MLs) at different spot positions. A Jobin Yvon-Horiba T64000 Raman spectrometer fitted with a charge-coupled device camera for the detection was used. All measurements were done in the backscattering configuration, using the 514.5 nm line of an Ar-Kr laser for excitation. The incident power on the sample was kept below 1 mW and a 100× focusing microscope objective was used, resulting in a ~1-μm-diameter spot. Spectra collected at different spot positions on the sample surface are shown in Fig. 2 along with a reference spectrum acquired on the 4*H*-SiC surface of the untreated sample. All Raman spectra collected on the graphitized sample surface show the characteristic 2*D* and *G* peaks, which confirm the presence of graphene, with the latter superimposed to the background signal associated with the substrate. Notice that the graphene fingerprint varies from spot to spot position. This is because, on such off-axis samples, the growth is still far from being optimized and the Raman spectra evidence a nonuniform coverage, with EG thickness varying rapidly at the micrometer scale. After the correction for the background signal, the number of (local) graphene MLs was estimated[17] with average values varying from 1 (or slightly less than 1) to 8 MLs. This is about three times the value found for

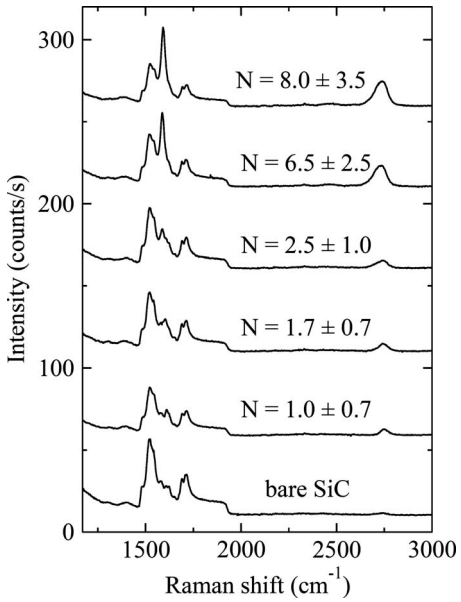

FIG. 2. Micro-Raman spectra collected on several positions on the EG sample. The spectrum on the bare (not thermally treated) 4*H*-SiC is also reported for reference.

on-axis (0001) 6*H*-SiC substrates;[5] but the nice point is that, at the micrometer scale, *no* region was found without any graphene sheet on top. Of course, since the Raman values are average coverage over the spot area, a ML thickness lower than 1 ML simply means incomplete graphene coverage.

To get more local information on the graphene coverage, with higher (submicrometer) resolution, TR-CAFM scans were performed at different tip positions on EG. Figure 3 shows a representative TR-CAFM current map [Fig. 3(b)] along with the morphology collected on EG [Fig. 3(a)]. Evidently, the surface has large corrugations with a measured roughness of 16 nm, which is significantly higher than the 0.3 nm roughness of the pristine 4*H*-SiC substrate. This comes from the large step-bunching phenomenon commonly observed on off-axis SiC substrates after high-temperature annealing ($T > 1400$ °C). ML graphene grows on the SiC surface following these steps. By comparing the morphology and current maps, bright regions carrying homogeneous cur-

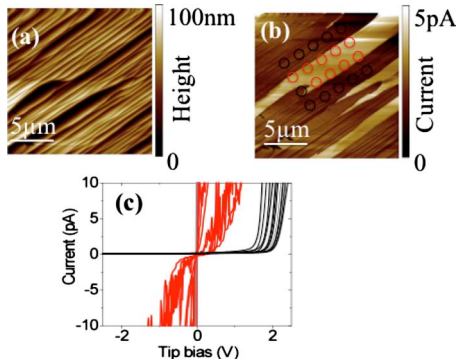

FIG. 3. (Color online) (a) Topography and (b) corresponding current map of EG on 4*H*-SiC (0001). The tip positions on regions covered by EG and on regions devoid of EG are indicated. The corresponding *I*-*V* curves are reported in (c).

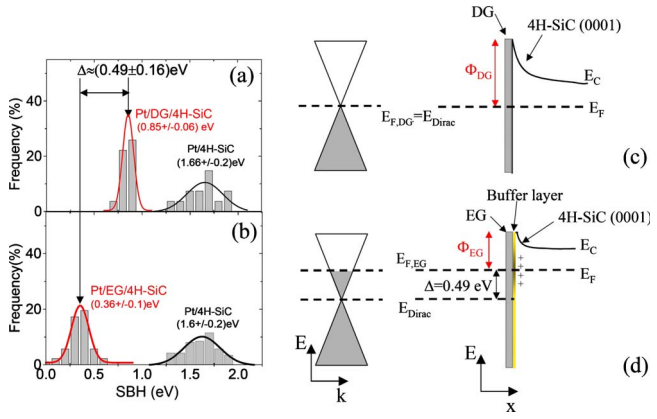

FIG. 4. (Color online) Histograms of SBHs evaluated for Pt/graphene/4*H*-SiC and Pt/4*H*-SiC in the cases of (a) DG and (b) EG. Corresponding band diagrams for DG and EG Schottky contacts on SiC are shown in (c) and (d), respectively.

rent in the current map appear evident. A comparison with the results obtained on DG suggests that these high carrying current areas are covered by a few MLs of graphene. To further analyze the interface current transport, we performed SCS and collected *I-V* characteristics in the same sample region. The results are shown in Fig. 3(c). Again, similar to the sample with DG, the *I-V* curves on the sample with EG can be divided into two distinct families: the curves acquired on an area covered with graphene and those acquired on an area free of graphene. The *I-V* characteristics on the graphene-free regions remained similar to those measured on the bare 4*H*-SiC surface in the sample not subjected to thermal treatment [see Fig. 1(b)]. On the opposite, the curves obtained on the regions coated with EG show completely different *I-V* characteristics. The leakage current is now very large with, in some cases, a clear Ohmic behavior. This is a direct evidence that the SBH at the EG/4*H*-SiC interface has been reduced with respect to DG/4*H*-SiC with, in some cases, a possibility of direct tunnel injection. These modified SBH (mSBH) values (due to the presence of graphene on SiC) have been evaluated for each of the *I-V* curves in Figs. 1(b) and 3(c), using the procedure of Refs. 14 and 15. The histograms of the corresponding values have been reported in Figs. 4(a) and 4(b), respectively. While the SBHs for Pt-tip/4*H*-SiC remain similar for both samples, the average mSBH value for EG on 4*H*-SiC appears very much reduced ($\Phi_{EG}=0.36\pm0.1$ eV) with respect to DG ($\Phi_{DG}=0.85\pm0.06$ eV). This fact is especially interesting considering that the SBHs on positions not covered with graphene remain similar. The SBH difference must then be explained in terms of the band diagrams schematically drawn in Figs. 4(c) and 4(d). Here, E_C is the energy of the conduction band edge, E_F is the Fermi energy at the bulk 4*H*-SiC, $E_{F,DG}$ is the Fermi energy of DG, and $E_{F,EG}$ the Fermi energy of EG. Due to the weak (van der Waals-like) interaction with the substrate, DG can be considered neutral (or close to neutral) in the absence of external bias. In this case, $E_{F,gr}$ should (more or less) coincide with the Dirac point energy (E_{Dirac}). Hence, in the first approximation, the SBH between DG and the *n*-type 4*H*-SiC epilayer should be given by the difference between the neutral graphene work function ($W_{gr}\approx4.5$ eV) (Ref. 18) and the 4*H*-SiC electron affinity ($\chi_{4H\text{-SiC}}\approx3.7$ eV).[19] We find 0.85 eV, instead of 0.8 eV, predicted by the simple model, and this supports completely our assumptions. The mSBH in the case of EG can now be explained in terms of a pinning of $E_{F,EG}$ at an average value $\Delta\sim0.49$ eV higher than $E_{F,DG}$, as shown in Fig. 4(d). As already said, for the sake of simplicity, we assumed neutral DG. This is only a first-order approximation but, in any case, the direct consequence is a reduction in W_{gr} by the Fermi energy difference Δ. This pinning is a direct evidence of the presence of positively charged states located at the interface between the Si face of 4*H*-SiC and C-rich $(6\sqrt{3}\times6\sqrt{3})R30°$ reconstructed buffer layer. This is consistent with recent theoretical results[20] showing, by electronic structure calculations of EG nanoribbons on (0001) SiC, a pinning of the Fermi level in the conduction band due to interface dangling bonds. This is also consistent with recent measurements of EG band structure by angle-resolved photoelectron spectroscopy (ARPES), showing a ~0.4 eV shift of the Fermi level with respect to the Dirac point, resulting in *n*-type doping of the graphene layers.[21] Macroscopic measurements of the SBH between thin graphite films and the Si face (on axis and 8° off axis) or C face of 4*H*- and 6*H*-SiC have been also reported,[22] for different dopant concentrations of the substrate (from 10^{16} to 10^{18} cm^{-3}). For lowest doping levels the SBH was determined by *I-V* and *C-V* measurements on test structures, whereas for highest concentrations, photoemission spectroscopy (PES) was applied. For graphite/4*H*-SiC (0001) the reported SBH by PES is 0.6 ± 0.1 eV, in agreement with the value obtained by *C-V* measurements (0.59 eV), while the SBH obtained by *I-V* curves is 0.4 eV.

However, ARPES, PES, macroscopic electrical measurements, and Raman spectroscopy give average values over the investigated area. Only scanning probe techniques can give nanoscale resolution information, like the evidence of a nonuniform energy distribution for the interface states. Focusing on the spread of mSBH values for EG/4*H*-SiC and using standard expressions for the two-dimensional density of states of graphene, we find that the average value is $\sim1.8\times10^{13}$ cm^{-2}, with extreme (local) values varying from about $\sim1\times10^{12}$ to $\sim5\times10^{13}$ cm^{-2} at a few μm distance. Such significant local inhomogeneities are in part due to the peculiar growth mechanism of EG on the off-axis 4*H*-SiC epilayer. A better understanding of this mechanism is necessary, also in view of integrating EG electronics with SiC devices (commonly fabricated on low-doped off-axis epilayers) for future rf applications. To conclude, we performed nanoscale current transport studies on graphene on an n^- (0001) 4*H*-SiC substrate using scanning current spectroscopy. Graphene deposited on SiC and graphene grown epitaxially on SiC have been examined, focusing on the interfacial electrical properties. Due to Fermi-level pinning toward the conduction band, a reduced SBH has been observed on EG as compared to DG. This effect shows that positively charged states localize at the interface between the C-rich $(6\sqrt{3}\times6\sqrt{3})R30°$ reconstructed buffer layer and the Si face. The energy distribution of these states has been found nonuniform and varying rapidly at the nanoscale.

*filippo.giannazzo@imm.cnr.it

[1] A. K. Geim, Science **324**, 1530 (2009).
[2] A. H. Castro Neto, F. Guinea, N. M. R. Peres, K. S. Novoselov, and A. K. Geim, Rev. Mod. Phys. **81**, 109 (2009).
[3] K. S. Novoselov, A. K. Geim, S. V. Morozov, D. Jiang, Y. Zhang, S. V. Dubonos, I. V. Grigorieva, and A. A. Firsov, Science **306**, 666 (2004).
[4] C. Berger, Z. Song, X. Li, X. Wu, N. Brown, C. Naud, D. Mayou, T. Li, J. Hass, A. N. Marchenkov, E. H. Conrad, P. N. First, and W. A. de Heer, Science **312**, 1191 (2006).
[5] C. Virojanadara, M. Syvajarvi, R. Yakimova, L. I. Johansson, A. A. Zakharov, and T. Balasubramanian, Phys. Rev. B **78**, 245403 (2008).
[6] K. V. Emtsev, A. Bostwick, K. Horn, J. Jobst, G. L. Kellogg, L. Ley, J. L. McChesney, T. Ohta, S. A. Reshanov, J. Rohrl, E. Rotenberg, A. K. Schmid, D. Waldmann, H. B. Weber, and T. Seyller, Nature Mater. **8**, 203 (2009).
[7] G. Gu, S. Nie, R. M. Feenstra, R. P. Devaty, W. J. Choyke, W. K. Chan, and M. G. Kane, Appl. Phys. Lett. **90**, 253507 (2007).
[8] Y. Q. Wu, P. D. Ye, M. A. Capano, Y. Xuan, Y. Sui, M. Qi, J. A. Cooper, T. Shen, D. Pandey, G. Prakash, and R. Reifenberger, Appl. Phys. Lett. **92**, 092102 (2008).
[9] J. Kedzierski, P. Hsu, P. Healy, P. Wyatt, C. Keast, M. Sprinkle, C. Berger, and W. de Heer, IEEE Trans. Electron Devices **55**, 2078 (2008).
[10] A. Mattausch and O. Pankratov, Phys. Rev. Lett. **99**, 076802 (2007).
[11] F. Varchon, R. Feng, J. Hass, X. Li, B. N. Nguyen, C. Naud, P. Mallet, J.-Y. Veuillen, C. Berger, E. H. Conrad, and L. Magaud, Phys. Rev. Lett. **99**, 126805 (2007).
[12] K. V. Emtsev, F. Speck, Th. Seyller, L. Ley, and J. D. Riley, Phys. Rev. B **77**, 155303 (2008).
[13] K. V. Emtsev, Th. Seyller, F. Speck, L. Ley, P. Stojanov, J. D. Riley, and R. C. G. Leckey, Mater. Sci. Forum **556-557**, 525 (2007).
[14] F. Giannazzo, F. Roccaforte, V. Raineri, and S. F. Liotta, EPL **74**, 686 (2006).
[15] F. Giannazzo, F. Roccaforte, F. Iucolano, V. Raineri, F. Ruffino, and M. G. Grimaldi, J. Vac. Sci. Technol. B **27**, 789 (2009).
[16] F. Giannazzo, S. Sonde, V. Raineri, and E. Rimini, Nano Lett. **9**, 23 (2009).
[17] N. Camara, J.-R. Huntzinger, G. Rius, A. Tiberj, N. Mestres, F. Perez-Murano, P. Godignon, and J. Camassel, Phys. Rev. B **80**, 125410 (2009).
[18] G. Giovannetti, P. A. Khomyakov, G. Brocks, V. M. Karpan, J. van den Brink, and P. J. Kelly, Phys. Rev. Lett. **101**, 026803 (2008).
[19] H. Na, H. Kim, K. Adachi, N. Kiritani, S. Tanimoto, H. Okushi, and K. Arai, J. Electron. Mater. **33**, 89 (2004).
[20] I. Deretzis and A. La Magna, Appl. Phys. Lett. **95**, 063111 (2009).
[21] T. Ohta, A. Bostwick, T. Seyller, K. Horn, and E. Rotenberg, Science **313**, 951 (2006).
[22] S. A. Reshanov, K. V. Emtsev, F. Speck, K.-Y. Gao, T. K. Seyller, G. Pensl, and L. Ley, Phys. Status Solidi B **245**, 1369 (2008).